Cell Reports, Volume *39*

Supplemental information

A TET1-PSPC1-*Neat1* molecular axis modulates PRC2 functions in controlling stem cell bivalency

Xin Huang, Nazym Bashkenova, Yantao Hong, Cong Lyu, Diana Guallar, Zhe Hu, Vikas Malik, Dan Li, Hailin Wang, Xiaohua Shen, Hongwei Zhou, and Jianlong Wang

Figure S1

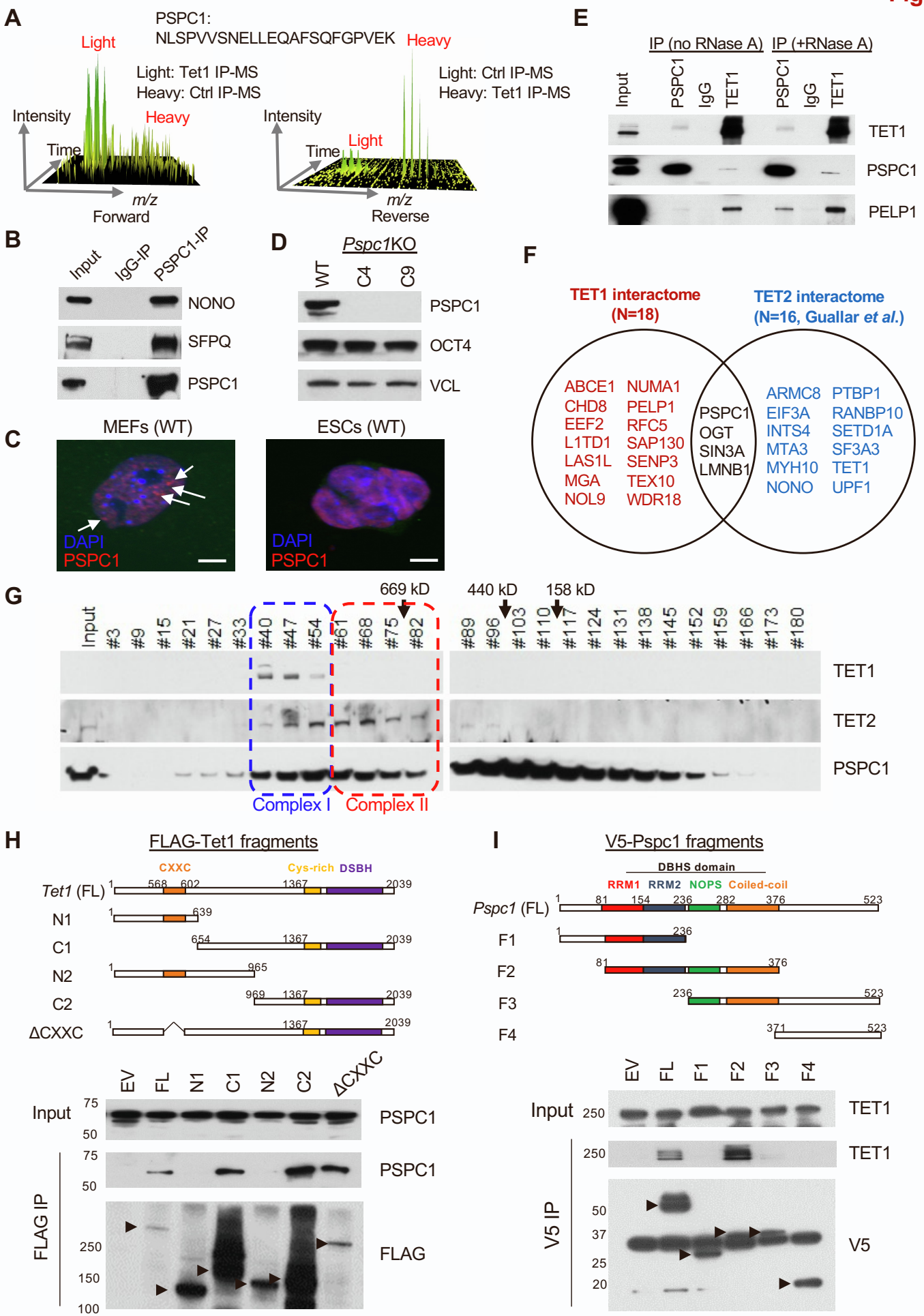
A
PSPC1:
NLSPVVSNELLEQAFSQFGPVEK
Light
Heavy
Light: Tet1 IP-MS
Heavy: Ctrl IP-MS
Light: Ctrl IP-MS
Heavy: Tet1 IP-MS
Intensity
Time
m/z
Forward
Reverse
B
Input
IgG-IP
PSPC1-IP
NONO
SFPQ
PSPC1
C
MEFs (WT)
ESCs (WT)
DAPI
PSPC1
D
Pspc1KO
WT
C4
C9
PSPC1
OCT4
VCL
E
IP (no RNase A)
IP (+RNase A)
Input
PSPC1
IgG
TET1
TET1
PSPC1
PELP1
F
TET1 interactome
(N=18)
TET2 interactome
(N=16, Guallar et al.)
ABCE1
CHD8
EEF2
L1TD1
LAS1L
MGA
NOL9
NUMA1
PELP1
RFC5
SAP130
SENP3
TEX10
WDR18
PSPC1
OGT
SIN3A
LMNB1
ARMC8
EIF3A
INTS4
MTA3
MYH10
NONO
PTBP1
RANBP10
SETD1A
SF3A3
TET1
UPF1
G
669 kD
440 kD
158 kD
Input
#3
#9
#15
#21
#27
#33
#40
#47
#54
#61
#68
#75
#82
#89
#96
#103
#110
#117
#124
#131
#138
#145
#152
#159
#166
#173
#180
TET1
TET2
PSPC1
Complex I
Complex II
H
FLAG-Tet1 fragments
CXXC
Cys-rich
DSBH
Tet1 (FL)
N1
C1
N2
C2
ΔCXXC
EV
FL
N1
C1
N2
C2
ΔCXXC
Input
PSPC1
FLAG IP
PSPC1
FLAG
I
V5-Pspc1 fragments
DBHS domain
RRM1
RRM2
NOPS
Coiled-coil
Pspc1 (FL)
F1
F2
F3
F4
EV
FL
F1
F2
F3
F4
Input
TET1
V5 IP
TET1
V5

Figure S1. Identification of PSPC1 as a novel partner of TET1 in ESCs. Related to Figure 1.

(A) SILAC quantification of a PSPC1 peptide NLSPVVSNELLEQAFSQFGPVEK by mass spectrometry. Quantification is based on the intensity from two replicates with reciprocal heavy/light labeling of FLAG-IP (TET1) and Control-IP (empty vector) MS experiments.

(B) Co-IP of PSPC1 and paraspeckle proteins NONO, SFPQ in ESCs, detected by western blot analysis of the antibodies against those proteins. IgG-IP serves as the negative control.

(C) Microscopy immunostaining images of WT MEFs and ESCs for PSPC1 (red) and DAPI (blue). The white arrows indicate paraspeckles. Scale bar, 5 μM.

(D) PSPC1 knockout *(Pspc1KO*) (two independent clones, C4 and C9) does not affect OCT4 levels in ESCs. VCL (Vinculin) serves as a loading control.

(E) Co-IP validation between endogenous TET1 and PSPC1 with and without RNase A treatment.

(F) Comparison of the TET1 (this study) and TET2 interactome (Guallar et al., 2018) identified in ESCs.

(G) Gel filtration assay for the co-fractionation of TET1, TET2, and PSPC1 in ESCs. Two potential protein complexes: Complex I (in the blue rectangle) containing TET1/TET2/PSPC1 and Complex II (in the red rectangle) containing TET2/PSPC1 are indicated.

(H) Domain mapping of Tet1 variants that interact with wildtype PSPC1. FLAG-tagged full length (FL) and different variants of Tet1 are indicated on top. Co-IP is performed with FLAG-IP of TET1 fragments followed by western blot analysis of PSPC1. The black arrows on the bottom show the correct size of expressed TET1 protein fragments. Empty vector (EV) serves as the negative control. DSBH denotes the double strain B helix domain of TET1.

(I) Domain mapping of Pspc1 variants that interact with wildtype TET1. V5-tagged full-length (FL) and different variants of Pspc1 are indicated on top. Co-IP is performed with V5-IP of PSPC1 fragments followed by western blot analysis of TET1. Note that there is a nonspecific band of V5 at 35 KDa. The black arrows on the bottom indicate the correct size of expressed PSPC1 variants. DBHS (drosophila behavior/human splicing), RRM (RNA recognition motifs), and NOPS (NonA/paraspeckle) domains of PSPC1 are indicated. Empty vector (EV) serves as the negative control.

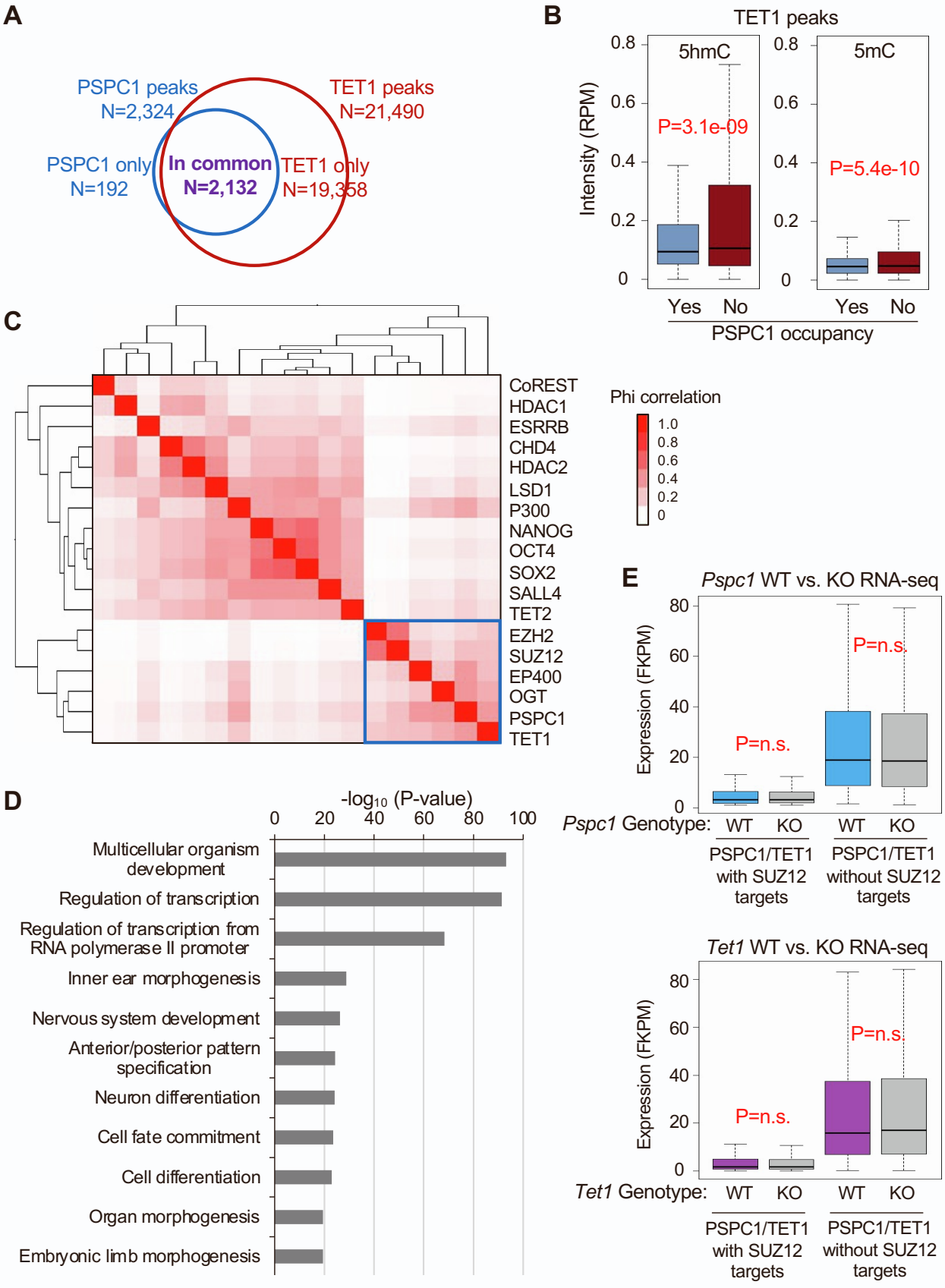
A
PSPC1 peaks
N=2,324
TET1 peaks
N=21,490
PSPC1 only
N=192
In common
N=2,132
TET1 only
N=19,358
B
TET1 peaks
5hmC
5mC
Intensity (RPM)
P=3.1e-09
P=5.4e-10
Yes
No
PSPC1 occupancy
C
CoREST
HDAC1
ESRRB
CHD4
HDAC2
LSD1
P300
NANOG
OCT4
SOX2
SALL4
TET2
EZH2
SUZ12
EP400
OGT
PSPC1
TET1
Phi correlation
D
-log10 (P-value)
Multicellular organism development
Regulation of transcription
Regulation of transcription from RNA polymerase II promoter
Inner ear morphogenesis
Nervous system development
Anterior/posterior pattern specification
Neuron differentiation
Cell fate commitment
Cell differentiation
Organ morphogenesis
Embryonic limb morphogenesis
E
Pspc1 WT vs. KO RNA-seq
Expression (FKPM)
P=n.s.
Pspc1 Genotype:
WT
KO
PSPC1/TET1 with SUZ12 targets
PSPC1/TET1 without SUZ12 targets
Tet1 WT vs. KO RNA-seq
Tet1 Genotype:

Figure S2. PSPC1, TET1, and PRC2 co-localize at the bivalent gene promoters in ESCs. Related to Figure 2.

(A) Overlap of the PSPC1 and TET1 ChIP-seq peaks in ESCs.

(B) Boxplots depicting quantification of DNA 5hmC and 5mC intensity at TET1 peak regions with or without PSPC1 occupancy. P-value is from the Mann-Whitney test. DNA 5hmC and 5mC DIP-seq data in ESCs are curated from (Xiong et al., 2016).

(C) ChIP-seq correlation analysis based on identified peaks of pluripotency-related transcription factors and epigenetic regulators in ESCs. A blue rectangle indicates TET1 ChIP-seq peaks are associated with its interacting partner PSPC1 and PRC2 subunits EZH2 and SUZ12.

(D) Gene ontology (GO) analysis for the PSPC1/TET1/SUZ12 common target genes.

(E) Boxplots depicting expression of the PSPC1/TET1 target genes with or without SUZ12 occupancy upon knockout (KO) of *Pspc1* (this study) or *Tet1* (Hon et al., 2014) in ESCs. P-value is from the Mann-Whitney test, and “n.s.” denotes statistically non-significant.

Figure S3

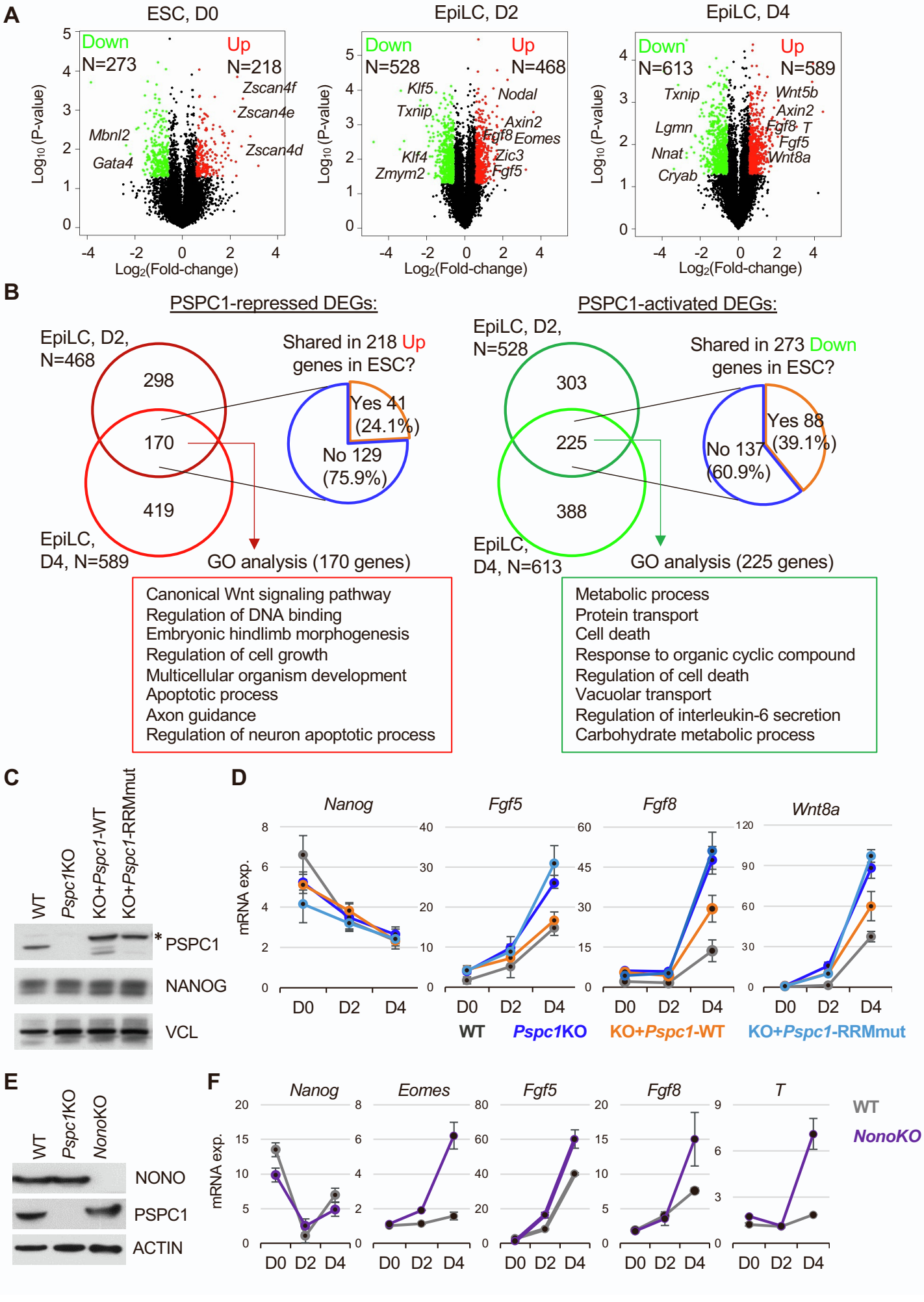
A
ESC, D0
Down
N=273
Up
N=218
Zscan4f
Zscan4e
Zscan4d
Mbnl2
Gata4
EpiLC, D2
Down
N=528
Up
N=468
Klf5
Txnip
Nodal
Axin2
Fgf8
Eomes
Zic3
Klf4
Zmym2
Fgf5
EpiLC, D4
Down
N=613
Up
N=589
Txnip
Wnt5b
Axin2
Lgmn
Fgf8
T
Fgf5
Nnat
Wnt8a
Cryab
Log10 (P-value)
Log2(Fold-change)
B
PSPC1-repressed DEGs:
EpiLC, D2, N=468
298
170
419
EpiLC, D4, N=589
Shared in 218 Up genes in ESC?
Yes 41 (24.1%)
No 129 (75.9%)
GO analysis (170 genes)
Canonical Wnt signaling pathway
Regulation of DNA binding
Embryonic hindlimb morphogenesis
Regulation of cell growth
Multicellular organism development
Apoptotic process
Axon guidance
Regulation of neuron apoptotic process
PSPC1-activated DEGs:
EpiLC, D2, N=528
303
225
388
EpiLC, D4, N=613
Shared in 273 Down genes in ESC?
Yes 88 (39.1%)
No 137 (60.9%)
GO analysis (225 genes)
Metabolic process
Protein transport
Cell death
Response to organic cyclic compound
Regulation of cell death
Vacuolar transport
Regulation of interleukin-6 secretion
Carbohydrate metabolic process
C
WT
Pspc1KO
KO+Pspc1-WT
KO+Pspc1-RRMmut
*
PSPC1
NANOG
VCL
D
Nanog
Fgf5
Fgf8
Wnt8a
mRNA exp.
D0
D2
D4
WT
Pspc1KO
KO+Pspc1-WT
KO+Pspc1-RRMmut
E
WT
Pspc1KO
NonoKO
NONO
PSPC1
ACTIN
F
Nanog
Eomes
Fgf5
Fgf8
T
mRNA exp.
WT
NonoKO

Figure S3. PSPC1 and NONO negatively regulate bivalent gene activation in pluripotent state transition. Related to Figure 3.

(A) Volcano plots depicting the differentially expressed genes (DEGs, P-value<0.05, fold-change>1.5) by comparing the WT and *Pspc1*KO cells at 3 time points (D0, D2, D4). Numbers of Down- and Up-regulated DEGs and some representative genes names are indicated.

(B) Pie charts depicting the overlap of the PSPC1-repressed (left) and -activated (right) DEGs in D2 and D4 EpiLCs. The numbers and percentages are indicated if these DEGs are also repressed (left) or activated (right) by PSPC1 in ESCs.

(C) Verification of PSPC1 expression in WT and *Pspc1*KO ESCs, and *Pspc1*KO ESCs rescued with a PSPC1 WT or an RNA recognition motif mutant (RRMmut) protein. *The two rescued proteins contain a FLAG tag. Therefore, their molecular weights are slightly above the endogenous PSPC1 band in WT cells. VCL (Vinculin) serves as a loading control.

(D) RT-qPCR analysis of *Nanog* and lineage genes (*Fgf5, Fgf8, Wnt8a*) in WT, *Pspc1*KO, and KO ESCs rescued with WT or RRMmut protein during EpiLC differentiation. Error bars represent the standard deviation of technical triplicates.

(E) Verification of the KO statuses of *Pspc1*KO and *Nono*KO ESCs by western blot analysis.

(F) RT-qPCR analysis of *Nanog* and lineage genes (*Eomes, Fgf5, Fgf8, T*) in WT and *Nono*KO ESCs during EpiLC differentiation. Error bars represent the standard deviation of technical triplicates.

Figure S4

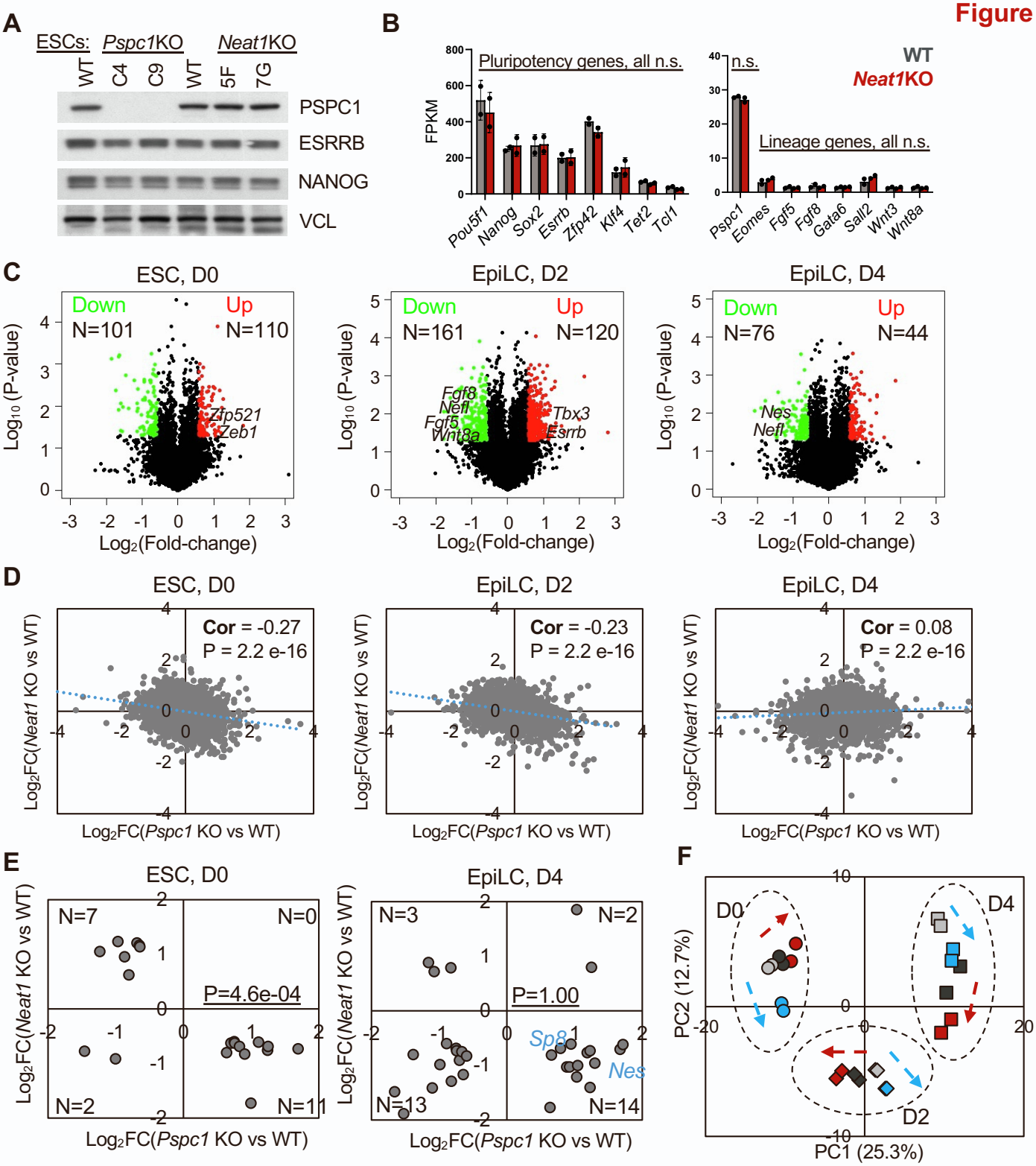
A
ESCs: Pspc1KO Neat1KO
WT C4 C9 WT 5F 7G
PSPC1
ESRRB
NANOG
VCL
B
Pluripotency genes, all n.s.
FPKM
Pou5f1 Nanog Sox2 Esrrb Zfp42 Klf4 Tet2 Tcl1
n.s.
WT
Neat1KO
Lineage genes, all n.s.
Pspc1 Eomes Fgf5 Fgf8 Gata6 Sall2 Wnt3 Wnt8a
C
ESC, D0
EpiLC, D2
EpiLC, D4
Down N=101
Up N=110
Down N=161
Up N=120
Down N=76
Up N=44
Log10 (P-value)
Log2(Fold-change)
Zfp521
Zeb1
Fgf8
Nefl
Fgf5
Wnt8a
Tbx3
Esrrb
Nes
Nefl
D
ESC, D0
EpiLC, D2
EpiLC, D4
Cor = -0.27
P = 2.2 e-16
Cor = -0.23
P = 2.2 e-16
Cor = 0.08
P = 2.2 e-16
Log2FC(Neat1 KO vs WT)
Log2FC(Pspc1 KO vs WT)
E
ESC, D0
EpiLC, D4
N=7
N=0
P=4.6e-04
N=2
N=11
N=3
N=2
P=1.00
Sp8
Nes
N=13
N=14
Log2FC(Neat1 KO vs WT)
Log2FC(Pspc1 KO vs WT)
F
D0
D4
D2
PC2 (12.7%)
PC1 (25.3%)
Pspc1WT
Pspc1KO
Neat1WT
Neat1KO
ESC, D0
EpiLC, D2
EpiLC, D4
G
Neat1_2
Neat1_1
Neat1 WT
ESC, D0 Input
Neat1 ChIRP
EpiLC, D2 Input
Neat1 ChIRP
Neat1 KO
ESC, D0 Input
Neat1 ChIRP
EpiLC, D2 Input
Neat1 ChIRP
H
Sfi1
PSPC1
TET1
SUZ12
ChIP (ESC)
Neat1 ChIRP

Figure S4. *Neat1* positively regulates the activation of bivalent genes in pluripotent state transition. Related to Figure 4.

(A) Western blot analysis of pluripotent stem cell factors ESRRB and NANOG in *Pspc1*KO (two independent clones, C4 and C9) and *Neat1*KO (two independent clones, 5F and 7G) ESCs. VCL (Vinculin) serves as a loading control.

(B) Histograms of expression shown in FPKM (fragments per kilobase of transcript per million mapped reads) values for the representative pluripotency and lineage genes in WT and *Neat1*KO ESCs. P-value is from the two-tailed T-test comparing the WT and *Neat1*KO values of each gene, and "n.s." denotes non-significant. Error bars represent the standard deviation of biological duplicates.

(C) Volcano plots depicting the DEGs by comparing the WT and *Neat1*KO cells at 3 time points (D0, D2, D4). Numbers of Down- and Up-regulated DEGs and some representative genes names are indicated.

(D) Scatter plots depicting the relative expression of all genes upon the loss of *Pspc1* (*Pspc1* KO/WT) or *Neat1* (*Neat1* KO/WT) at 3 time points (D0, D2, D4). The Pearson's product-moment correlation coefficient (*r*) and P-value of correlation are indicated in each plot.

(E) Scatter plots depicting the relative gene expression of DEGs (P-value<0.05, fold-change>1.5) upon the loss of *Pspc1* (*Pspc1* KO/WT) or *Neat1* (*Neat1* KO/WT) in ESCs (left) and D4 EpiLCs (right) from RNA-seq analysis. P-value is from the Fisher-extract test.

(F) Principal component analysis (PCA) of *Pspc1* WT and KO, *Neat1* WT and KO RNA-seq samples at different time points (D0, D2, D4). Percentages of variance explained in each principal component (PC) are indicated. The arrows indicate the trend of gene expression changes comparing the KO vs. WT samples at 3 time points.

(G-H) *Neat1* ChIRP-seq tracks in WT and *Neat1*KO ESCs and D2 EpiLCs at the *Neat1* (G) and *Sfi1* (H) loci. The PSPC1, TET1, and SUZ12 ChIP-seq tracks in ESCs are also shown at the *Sfi1* (H) locus. The numbers indicate the normalized RPM value of the tracks.

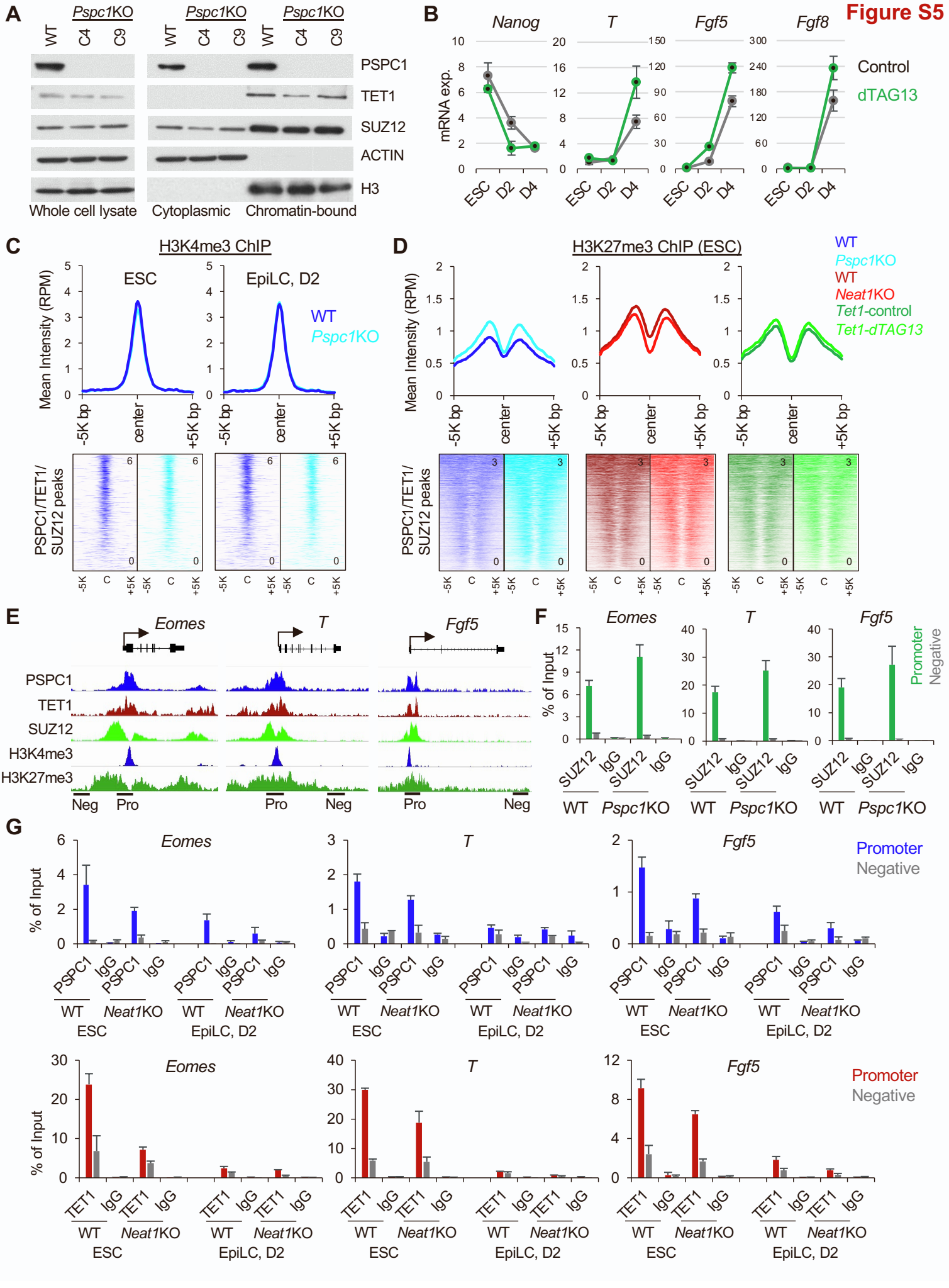
Figure S5
A
Pspc1KO
WT
C4
C9
PSPC1
TET1
SUZ12
ACTIN
H3
Whole cell lysate
Cytoplasmic
Chromatin-bound
B
Nanog
T
Fgf5
Fgf8
mRNA exp.
ESC
D2
D4
Control
dTAG13
C
H3K4me3 ChIP
ESC
EpiLC, D2
Mean Intensity (RPM)
WT
Pspc1KO
-5K bp
center
+5K bp
PSPC1/TET1/
SUZ12 peaks
D
H3K27me3 ChIP (ESC)
WT
Pspc1KO
WT
Neat1KO
Tet1-control
Tet1-dTAG13
E
Eomes
T
Fgf5
PSPC1
TET1
SUZ12
H3K4me3
H3K27me3
Neg
Pro
F
% of Input
Promoter
Negative
SUZ12
IgG
WT
Pspc1KO
G
PSPC1
TET1
WT
Neat1KO
ESC
EpiLC, D2
Promoter
Negative

Figure S5. Depletion of PSPC1 or TET1 accelerates PRC2 eviction from bivalent gene promoters. Related to Figure 5.

(A) Western blot analysis of whole-cell lysate, cytoplasmic, and chromatin-bound fractions of PSPC1, TET1, and SUZ12 in WT and *Pspc1*KO (two independent clones, C4 and C9) ESCs. ACTIN and histone H3 are the loading controls of cytoplasmic and chromatin-bound fractions, respectively.

(B) RT-qPCR analysis of the pluripotency gene (*Nanog*) and lineage genes (*T, Fgf5, Fgf8*) in *Tet1*-degron ESCs treated with control DMSO or dTAG-13 during EpiLC differentiation. Error bars represent the standard deviation of technical triplicates.

(C) Mean intensity plot (top) and heatmap (bottom) by RPM of H3K4me3 ChIP-seq intensity upon *Pspc1*KO in ESCs and D2 EpiLCs at the PSPC1/TET1/SUZ12 common peak regions (within 5K bp at the peak center, identified in ESCs).

(D) Mean intensity plot (top) and heatmap (bottom) by RPM of H3K27me3 ChIP-seq intensity of different genotypes (*Pspc1* WT/KO, *Neat1* WT/KO) or treatment (*Tet1*-degron with DMSO-control/dTAG13) in ESCs at the PSPC1/TET1/SUZ12 common peak regions (within 5K bp at peak center, identified in ESCs).

(E) PSPC1, TET1, SUZ12, and bivalent marks H3K4me3 and H3K27me3 ChIP-seq tracks at bivalent promotes (*Eomes, T, Fgf5*) in ESCs. Primers for ChIP-qPCR analysis (Panels F, G) are designed at the promoter (Pro) and a nearby negative (Neg) region of each locus.

(F) ChIP-qPCR analysis of SUZ12 at bivalent promoters (*Eomes, T, Fgf5*, target sites shown in Panel E) in WT and *Pspc1*KO ESCs. Error bars represent the standard deviation of technical triplicates.

(G) ChIP-qPCR analysis of TET1 (top) and PSPC1 (bottom) at bivalent promoters (*Eomes, T, Fgf5*, target sites shown in Panel E) in WT and *Neat1*KO ESCs and D2 EpiLCs. Error bars represent the standard deviation of technical triplicates.

Figure S6

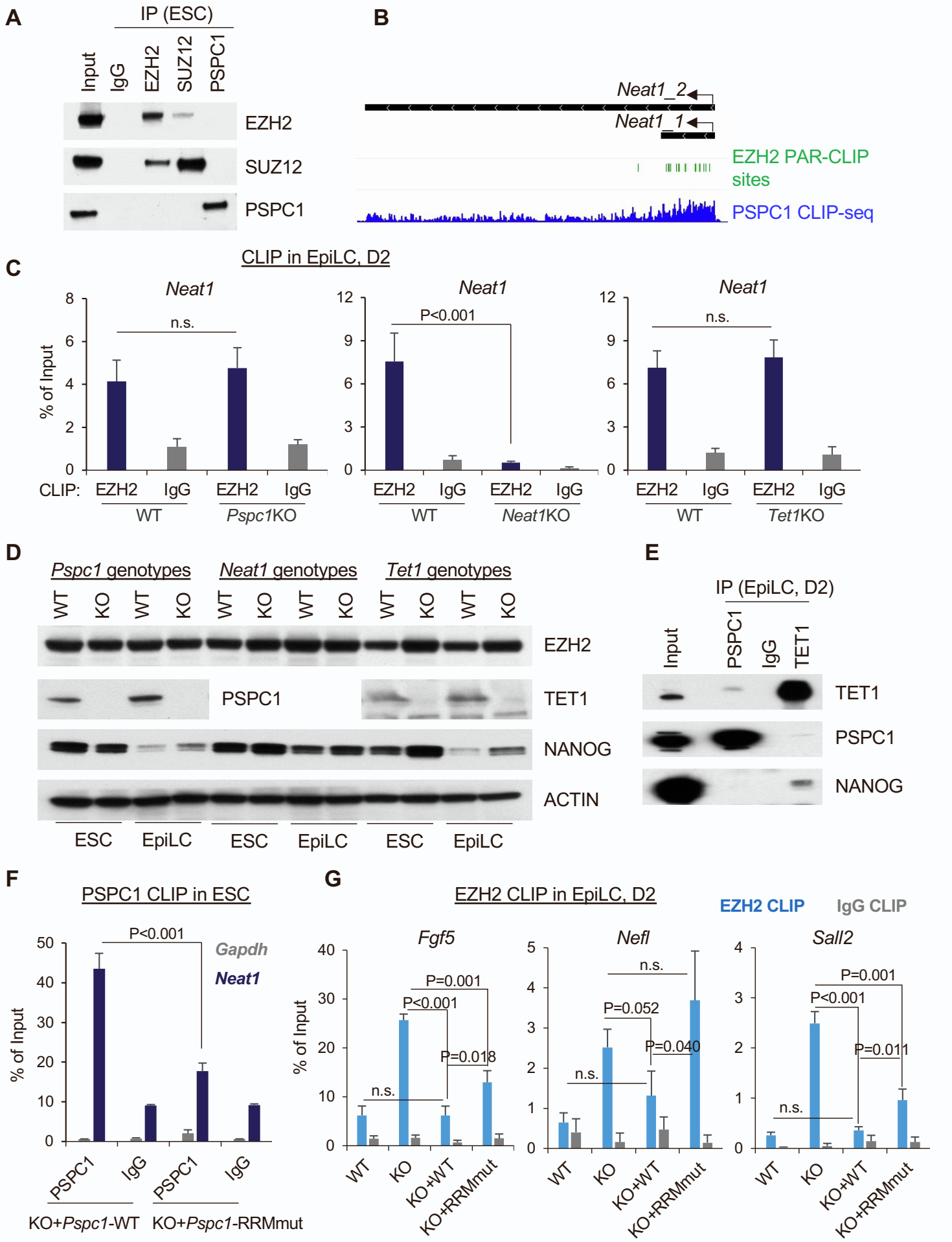
A
IP (ESC)
Input
IgG
EZH2
SUZ12
PSPC1
EZH2
SUZ12
PSPC1
B
Neat1_2
Neat1_1
EZH2 PAR-CLIP sites
PSPC1 CLIP-seq
C
CLIP in EpiLC, D2
Neat1
% of Input
n.s.
P<0.001
CLIP: EZH2 IgG EZH2 IgG
WT
Pspc1KO
Neat1KO
Tet1KO
D
Pspc1 genotypes
Neat1 genotypes
Tet1 genotypes
WT KO WT KO WT KO WT KO WT KO WT KO
EZH2
PSPC1
TET1
NANOG
ACTIN
ESC EpiLC ESC EpiLC ESC EpiLC
E
IP (EpiLC, D2)
Input
PSPC1
IgG
TET1
TET1
PSPC1
NANOG
F
PSPC1 CLIP in ESC
P<0.001
Gapdh
Neat1
% of Input
PSPC1 IgG PSPC1 IgG
KO+Pspc1-WT
KO+Pspc1-RRMmut
G
EZH2 CLIP in EpiLC, D2
EZH2 CLIP
IgG CLIP
Fgf5
Nefl
Sall2
% of Input
P=0.001
P<0.001
P=0.018
n.s.
P=0.052
P=0.040
P=0.011
WT KO KO+WT KO+RRMmut

Figure S6. PSPC1, TET1, and *Neat1* modulate PRC2 binding to nascent bivalent gene transcripts during bivalent gene activation. Related to Figure 6.

(A) The lack of physical association between PSPC1 and PRC2 under a nucleosome-free co-IP protocol. Co-IP of PSPS1 and PRC2 subunits EZH2 and SUZ12 was performed in ESCs using a nucleosome-free protocol (see details in Methods) followed by western blot analysis.

(B) Both EZH2 and PSPC1 bind to *Neat1* lncRNA. EZH2 PAR-CLIP-seq binding sites were processed from (Kaneko et al., 2013) and PSPC1 CLIP-seq was from (Guallar et al., 2018). The CLIP-seq tracks at *Neat1* locus in ESCs were indicated by green vertical lines (for EZH2) or peaks (for PSPC1).

(C) EZH2 CLIP-qPCR analysis of *Neat1* in *Pspc1* WT/KO, *Neat1* WT/KO, and *Tet1* WT/KO D2 EpiLCs. P-value is from 2-tailed T-test, and "n.s." denotes non-significant.

(D) EZH2 total proteins are not changed by the loss of *Pspc1*, *Neat1*, or *Tet1*, or during the ESC-to-EpiLC transition, confirmed by western blot analysis with indicated antibodies. PSPC1 was upregulated, while NANOG (a naïve marker) was notably downregulated in D2 EpiLCs relative to ESCs, although its levels are relatively unaffected in KO relative WT ESCs or D2 EpiLCs.

(E) Co-IP validation between endogenous TET1 and PSPC1 in D2 EpiLCs. NANOG also interacts with TET1 but not with PSPC1.

(F) PSPC1 CLIP-qPCR analysis of *Neat1* in *Pspc1*KO ESCs rescued with a PSPC1 WT or RRMmut protein. P-value is from the two-tailed T-test.

(G) EZH2 CLIP-qPCR analysis of bivalent genes' transcripts (*Fgf5, Nefl, Sall2*) in WT, *Pspc1*KO D2 EpiLCs, and KO cells rescued with a PSPC1 WT or RRMmut protein. P-value is from the two-tailed T-test.

Error bars in (C, F, G) represent the standard deviation of technical triplicates. Experiments were repeated in biological duplicates.